REVIEW PAPER

A survey of deep learning for MRI brain tumor segmentation methods: Trends, challenges, and future directions

Srigiri Krishnapriya[1] · Yepuganti Karuna[1]

Abstract

Purpose Structural Magnetic Resonance Imaging (MRI) of the brain is an effective way to study its internal structure. Identifying and classifying brain malignancies is a difficult and onerous task commonly handled by radiologists. Digital image processing processes, such as preprocessing, segmentation, and classification, can help clinical specialists diagnose certain types of brain cancers in addition to detecting the precise location of tumors and studying minute alterations. The state of brain tumor identification using MRI scans is discussed in this survey using numerous state-of-the-art machine learning and deep learning approaches.

Methods This review highlights brain tumor image segmentation techniques, publicly available datasets, deep learning techniques, and deep learning architectures used by various researchers in the process of brain tumor detection. Additionally, the study presents a comprehensive review of the performance of existing deep learning algorithms, challenges, and future research directions.

Results Various methods proposed so far have been compared based on their accuracy. Many studies have attained an accuracy of more than 98% using SVM in the segmentation and analysis of brain tumor detection using MR images. The ANN outperformed all the other algorithms with 99% accuracy in brain tumor detection using deep learning.

Conclusion This review's objective is to increase scholars' interest in this difficult field and familiarize them with current advancements in it. To create CAD systems aimed at brain tumor identification using MR images, digital image processing approaches, such as preprocessing, segmentation, and classification, are applied. The classic machine learning and deep learning approaches for brain tumor identification are deliberated in this work. This paper provides a summary of commonly used MR image datasets. For classification, various machine learning and deep learning algorithms have been used. This survey examines current methodologies and can be used in the future to develop effective diagnostic plans for other brain disorders such as dementia, Alzheimer's disease, stroke, and Parkinson's disease using various Magnetic Resonance imaging modalities.

Keywords Digital Image Processing · Machine learning · Deep learning · Structural Magnetic Resonance Imaging · Brain tumor detection

1 Introduction

A brain tumor occurs when cells proliferate irregularly in the brain or skull, and few tumors are benign others malignant [1]. Cancers may arise from the brain tissue itself (primary) or spread to the brain from elsewhere in the body(metastasis).

✉ Yepuganti Karuna
  karun@vit.ac.in

  Srigiri Krishnapriya
  srigiri.cheeki@gmail.com

1 School of Electronics Engineering, Vellore Institute of Technology, Vellore, India

Tumors of various sizes and types require different treatments. Regular cells grow in a precise manner as new cells substitute old or damaged cells.

Tumor cells replicate irrepressibly for reasons that are not yet fully understood. The term primary brain tumor refers to an anomalous development that originates in the brain and does not blow out to other portions of the body. Primary brain cancers can be benign or malignant. A benign tumor grows gradually, has different boundaries, and hardly spreads. Benign tumors, even though their cells are non-malignant, can be dangerous if they are positioned in a vital organ. Malignant tumors grow hastily, have uneven boundaries, and spread to neighboring brain areas.

The term "brain cancer" is often used; however malignant brain tumors are not suitable for the description of cancer because they do not blow out to other body parts.

Metastatic (secondary) brain tumors begin as cancer in places in the body and spread to the brain. The most common malignancies that blow out to the brain are the breasts and lungs. Bounded in the bony cranium, the brain cannot create an area with an increasing mass. As an outcome, the tumor constricts and dislocates into typical brain tissue. Some brain cancers form a jam of cerebrospinal fluid that flows from one location to another and across the brain. This obstruction increases the intracranial strain and can widen the ventricles (hydrocephalus). A few brain tumors can cause inflammation (edema). The Mass Effect which is original to many symptoms, is caused by size, pressure, and swelling. Malignant brain tumors encompass gliomas. These types of tumors arise in glial cells that mount and support the nerve cells. Gliomas account for two-thirds of malignant primary brain tumors [2]. Gliomas are classified as follows:

i. Astrocytoma: Astrocytomas are tumors that develop in glial cells known as astrocytes.
ii. Glioblastoma: Glioblastomas are aggressive astrocytomas that grow rapidly.
iii. Oligodendroglioma: These rare malignancies start in myelin-producing cells.
iv. Medulloblastoma: These tumors originate near the base of the skull and grow rapidly.

The process of tomography, the interior of a person for medical investigation and intrusion, as well as a graphical picture of the function of precise tissues, is referred to as medical imaging (physiology). The following is a general classification of brain imaging technologies based on the system's energy basis: (1) carotid Doppler and transcranial Doppler ultrasound; (2) X-ray images, which include angiography, computed tomography, and myelography; (3) magnetic fields, which include Magnetic Resonance Imaging (MRI), magnetoencephalography (MEG), Magnetic Resonance Spectroscopy (MRS), and magnetic resonance spectroscopic imaging (MRSI); (4) radioactivity, which encompasses Positron Emission Tomography (PET) and single-photon emission computed Tomography(SPECT); and (5) electrical activity including quantitative electro-encephalography (QEEG). Brain tomography procedures can also be categorized into structural and functional techniques. Anatomical areas were detected using structural techniques. Body structure and metabolism of the regions of interest were demonstrated using functional techniques. MRI, CT, Doppler, Angiography, and myelography are structural imaging methods. Functional imaging techniques include MEG, functional MRI (fMRI), MRS, QEEG, PET, and SPECT [3].

Magnetic Resonance Imaging (MRI) is a noninvasive imaging procedure that is generally applied in medical practice because it produces images with great spatial tenacity in addition to the high dissimilarity between soft tissues. For detailed analysis and treatment planning, MRI provides information regarding the size, shape, and location of brain tumors [4, 5]. T1-weighted, T2-weighted, fluid attenuated inversion recovery (FLAIR), and proton-density weighted are some of the MRI sequences that can be formed into weighted images. T1-weighted contrast-enhanced images and FLAIR are commonly used for brain tumor structure diagnosis because of the high contrast between gray and white matter [6].

Image segmentation is an emerging research area in medical imaging that entails extracting one or more sections from an image that forms the area of interest. Numerous algorithms have been developed in the literature to detect brain tumors, together with threshold-based approaches [7, 8], region-based methods [9, 10], deformable methods [11–14], classification methods [15, 16], and deep learning procedures [17–19].

This study is comprised of eight primary sections. Section 2 describes brain tumor segmentation approaches. The segmentation techniques are presented in Section 3. Section 4 discusses the deep learning architectures. The framework for deep learning development is presented in Section 5. Section 6 describes publicly accessible datasets. Section 7 presents a literature review. The analysis of this paper is presented in Section 8. The study is concluded in Section 9.

2 Brain tumor image segmentation approaches

The brain tumor segmentation process entails removing the tumor location from healthy brain tissues. However, because tumors can vary in size and location, effective segmentation remains a difficult task. They can have a non-rigid structure and complicated shape, as well as various appearance features. They have intensities that overlap with regular brain tissues, particularly at tumor borders [20], owing to the necessity to include physical data about the tumor to emphasize segmentation algorithms for more exact and effective extraction. Figure 1 depicts the brain segmentation of the normal tissues. Brain tumor segmentation approaches can be categorized as follows.

i. Manual segmentation method
ii. Semi automatic segmentation method
iii. Fully automatic segmentation method
iv. Hybrid segmentation method.

In the process of manual segmentation, the radiotherapist integrates the multimodal data provided through the

Fig. 1 Brain segmentation modules: (i) gray matter (GM), (ii) white matter (WM), (iii) cerebrospinal fluid (CSF) [21]

(i)   (ii)   (iii)
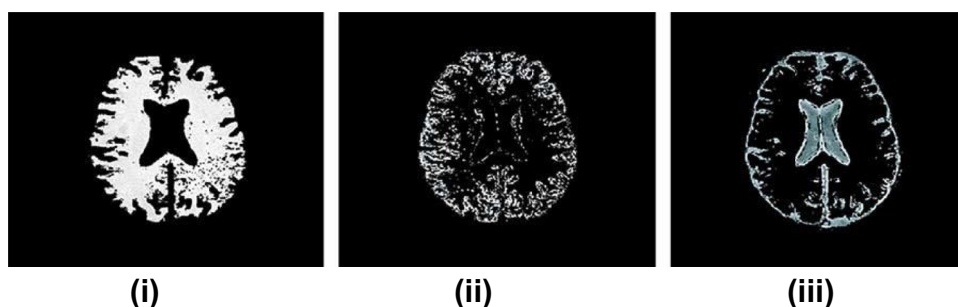
MR images with physiological and anatomical information acquired via training and practice. The radiologist must go through many parts of the images one by one, analyze the cancer, and carefully draw the tumor positions manually. Manual segmentation is both slow and radiologist-dependent [22]. It is frequently used to evaluate the outputs of semi-automated and completely automated systems.

In semi-automated techniques, user participation is necessary for three main goals: initialization, intervention, and evaluation [23]. In many circumstances, the automatic method is initiated by defining a region of interest (ROI) that roughly covers the tumor area. Apart from initialization, automated processes can be steered to the anticipated output by collecting responses and making essential adjustments. Additionally, if the user remains unhappy with the outcomes, the process can be adjusted or redone.

The "Tumor Cut" approach was anticipated by Hamamci et al. [24]. To use the semi-automated method, the extreme diameter of the tumor on the magnetic resonance image was sketched. A cellular automation-based seeded segmentation technique runs twice, once for user-supplied tumor seeds and again for background seeds, to produce a tumor probability map. This structure entails putting on the algorithm individual MRI modalities separately and then assimilating the findings to yield the ultimate tumor size.

A different classification procedure was used in the current semi-automatic method [25]. In this process, the segmentation-related problem is transformed into a classification problem. The tumor was segmented and classified solely inside the same brain. Machine learning algorithms for brain tumor segmentation generally require a large number of MRI scans from various cases to train. As a result, it is necessary to use an intensity bias correction. This method trains a support vector machine (SVM) to categorize all voxels in the same image to their respective tissue types by abstracting the intensity values and spatial coordinates as features for these subsets of voxels.

Semi-automated brain tumor segmentation procedures require less time and yield more accurate results than manual methods. As a result, the widely held current research on brain tumor segmentation is centered on fully automated means. Human involvement is not necessary in fully automated brain tumor segmentation systems. The segmentation problem is generally solved by combining artificial intelligence and prior knowledge. Hybrid segmentation combines various segmentation algorithms to achieve improved outcomes in terms of accuracy and computational time.

2.1 Conventional methods

Typical image processing approaches such as threshold-based approaches [26, 27] and region-based methods [28] are mostly used in traditional tumor segmentation procedures. Region-based and threshold-based methods are commonly used in two-dimensional image segmentation [29]. The various types of image segmentation techniques are presented in Figure 2.

2.1.1 Threshold-based methods

The threshold-based technique compares the intensities to one or more intensity thresholds and is an effective segmentation method. Currently, there are two types of threshold-based approaches: global and local thresholding. Global thresholding is the best method for segmenting objects and backgrounds when an image comprises objects of equal intensity or high contrast between the objects and background. Choosing a threshold when the contrast of an image is inadequate may be difficult. The intensity histogram can be used to determine the local thresholding by approximating a threshold value for distinct areas.

2.1.2 Region-based methods

To construct disjoint sections, region-based segmentation procedures examine pixels in an image and merge neighboring pixels using homogeneity features established on a preset similarity threshold [30]. The region-based methodology, employed in brain tumor segmentation, incorporates both region growth and watershed segmentation approaches.

Region growth is a region-based segmentation method that extracts a linked region of comparable pixels from the

Fig. 2 Types of Image Segmentation Techniques
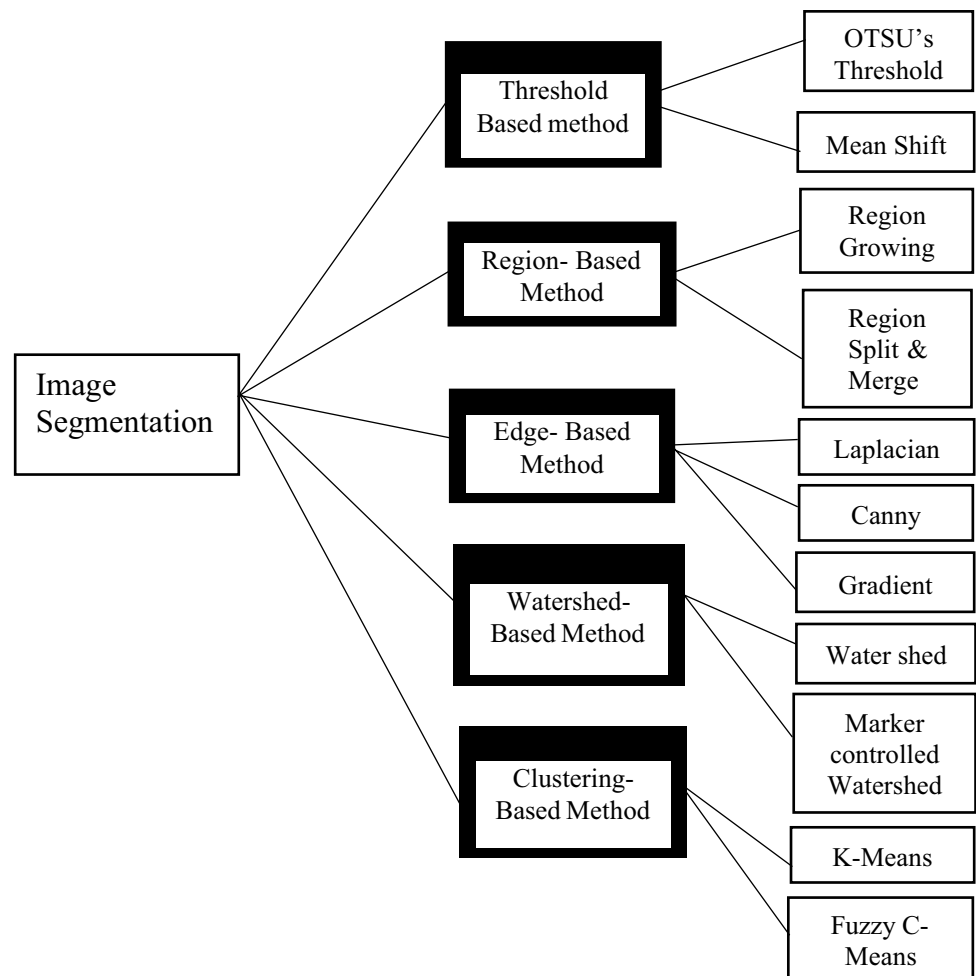
region of interest of at least one seed required to grow a region. The seed neighbors are verified, and those that meet the requirements for resemblance are added to the area. Seeds can be selected manually or automatically through a seed-finding process [31]. This process is repeated until there are no extra pixels to be added to the region. The benefit of region growth is that it can appropriately segment regions with comparable attributes and generate connected regions [32]. Some studies have demonstrated that region growth is a more effective and computationally efficient method of segmenting Magnetic Resonance images of brain tumors than other non-region-based methods, particularly for similar tissues and regions [33, 34].

The major drawback of the region-growth technique is the partial volume effect [35], which limits the accuracy of MRI brain segmentation. As a voxel denotes more than one type of tissue, the intensity difference among various tissue classes next to the boundary of the two tissue types is blurred by the partial volume effect [36]. The region-growing procedure is included as an enhancement phase in several segmentation systems [37]. A fuzzy information fusion context was proposed for MRI-based automatic brain tumor segmentation [38].

A metaphor created for water behavior in a landscape can be used to describe the basic principle behind the watershed segmentation approach. After rainfall, droplets of water from dissimilar areas shadow the descending landscape. Finally, the water reaches the lowest point of the valley. Each valley has a drainage zone in which all water flows. Dams are built at sites where water from separate basins meet. The procedure is halted when the level of water reaches the uppermost point in the terrain. Consequently, the landscape is separated into watershed lines or watersheds, which are regions separated by dams. To segment brain tumors, researchers have used multiscale watershed transformation [39, 40]. User-aided hierarchical watershed segmentation approaches for brain cancers using MRI data have been investigated [41]. Based on both qualitative and quantitative fallouts, the segmentation time and accuracy were significantly enhanced and exceeded those of manual segmentation. According to this study, the Watershed method for brain tumor segmentation has a few drawbacks.

Several approaches have been proposed to overcome these limitations. Ratan et al. [42] A multi-parameter watershed segmentation technique for the detection of tumors in 2D and 3D

cerebral MRI was suggested. For the segmentation of brain tumors, a marker-based enhanced watershed method with prior knowledge of test images was proposed [43]. Over-segmentation is a common problem in watershed segmentation methods. Some advanced algorithms have been developed [44–46] to avoid over-segmentation and generate appropriate segmentation. In summary, accurate brain tumor segmentation using traditional approaches is difficult to achieve. These approaches have been used as preprocessing steps in brain tumor segmentation in most cases. Hence, further advanced automatic procedures were projected to comply with clinical doctors' needs.

2.2 Classification and clustering methods

Machine learning is a useful method for systematizing medical image analyses and diagnoses. This might theoretically minimize the workload of radiologists in the practice of radiology [47], allowing them to examine complex correlations or patterns in experimental data and make accurate conclusions [48]. Distinct groups of machine-learning algorithms can be constructed based on various ideas. Based on the application of labels to training samples, this technique can be divided into supervised, unsupervised, and semi-supervised learning algorithms [49]. Each sample in supervised learning has two slices: features, input observations, and labels or output observations [50]. Generally, causes are observed in the input, whereas effects are observed in the output. Its principle is to create a practical relationship between the training and testing data. A combination of equations, weights, or numerical coefficients constitutes the relationship technique. Supervised learning is exemplified by a classification algorithm.

For each sample in unsupervised learning methods, there are a number of observations, but no label data [51]. These traits usually result from a set of unseen or latent causes. Unsupervised learning is used to identify hidden variables or correlations between the data. An example of an unsupervised learning method is clustering. Semi-supervised learning [52] associates with the benefits of both unsupervised and supervised learning. During the training process, both labeled and unlabeled information are used. Owing to the high cost and impossibility of labeling data in particular applications, semi-supervised learning methods have been developed [53]. Most brain cancer segmentation techniques are grounded on published clustering or classification procedures, such as Markov Random Fields (MRF), Fuzzy C-Means (FCM), k-means, Bayes, Support Vector Machine (SVM), Atlas-based, Artificial Neural Networks (ANN), and so on.

2.2.1 Fuzzy C-Means algorithms

FCM is a clustering technique that divides a single set of data into two or more clusters. Pattern recognition frequently uses this method [54]. This technique associates each data point identical to the respective cluster centers based on the distance between the data point and cluster. The data are more likely to be a member of the cluster center if it is close to it. Some of the advantages of the FCM approach are as follows: (1) It is comparable to the k-means method and delivers the best results for overlapping datasets. (2) Unlike k-means, which requires that each data point be assigned to only one cluster center, data points can be assigned to several cluster centers. Consequently, a single data point can be assigned to several cluster centers. (3) The use of FCM for MRI data yielded positive outcomes [55].

In a survey on brain tumor segmentation, active cells, necrotic cores, and edema were categorized into tissue classes using an unsupervised FCM clustering algorithm [56]. From the raw MR image data, this technique may produce segmentation images that convey therapeutically significant neuroanatomical and neuropathological tissue contrast information. Later, other researchers merged more data into feature vectors that were grouped together using FCM. The segmentation of brain tumors is predicted to be handled by a structure that associates knowledge-based approaches with multispectral histogram analysis [57]. Based on observations, the fuzzy clustering technique was aimed at the segmentation of brain tumor MR images, followed by 3-D linked mechanisms to determine the tumor outline [58]. Based on modified seeded region growing and fuzzy knowledge a new segmentation method called Fuzzy Knowledge-based Seeded Region Growing (FKSRG) was presented [59]. According to experimental results, the FKSRG approach slices multispectral MR images far more efficiently than the Automated Segmentation Means, k-means, and SVM algorithms.

Because FCM is a reiterative process, it is regarded as a labor-intensive clustering technique. Some methods, such as the corrected FCM (BCFCM) algorithm and Fast Generalized FCM (FGFCM) clustering algorithms have been designed to reduce the implementation time of this technique. FGFCM clustering methods incorporate local information and the FCM framework for the segmentation of brain tumors [60]. The BCFCM method quickly produces high-quality segmented brain images making it an ideal tool for assisting virtual brain endoscopy in the study of brain tumor segmentation [61].

The Particle Swarm Optimization (PSO) technique is an ideal solution, whereas Genetic Algorithms (GAs) are virtuous in achieving a nearby finest solution but struggle to discover a precise solution. The optimal value of the degree of attraction was determined using a combination of the GAs and PSO [62]. A union of the fuzzy C-means along with the k-means algorithm was presented to study brain tumor segmentation to increase the accuracy of tumor stage and size determination [63]. This method

allows for the accurate and repeatable segmentation of tumor tissue, analogous to manual segmentation.

2.2.2 Atlas‑based algorithm

The Atlas‑based technique was first used to list various images [64]. Subsequently, atlas‑based segmentation methods for directing brain tissue segmentation have been widely adopted. Atlases can be used to pinpoint the exact location of tumors and create productive classification models. An atlas‑based algorithm for brain tumor segmentation has three steps: first, the patient and the atlas are brought into global correspondence, then, a pattern for the brain tumor is provided by seeding an artificial tumor into the brain atlas, and finally, the seeded atlas is distorted by means of optical flow principles, and the brain cancer grows [65].

By altering an atlas with patient‑specific tumor location information from dissimilar Magnetic Resonance modalities [67, 68], brain tumors can be segmented with a tissue model in addition to the expectation‑maximization (EM) technique [66]. By incorporating earlier biomechanical [69] and shape [70] data into atlas‑based deformable registration, the methodologies in these two articles can be called atlas‑based approaches. The benefit of this approach is that domain knowledge can be combined with atlas‑based segmentation for improved consideration. Nevertheless, the inconsistency in such previous information is difficult to explain.

In the case of large space‑occupying tumors, a technique based on an a priori model of lesion development that undertakes the radial extension of the lesion from its initial position for brain atlas deformation was offered, and good segmentation results for brain tumors were obtained. These approaches restrict local intersubject anatomical variation, which results in less effective segmentation guidance. The slices of the results of the method are shown in Figure 3. Cabezas et al. [71] provided an overview of automated algorithms for segmenting magnetic resonance brain images using atlases. Recently, multimodal segmentation of gliomas using a probabilistic tissue model was accomplished using localization based on the brain atlas [72]. The key to an atlas‑based approach is a precise atlas. The efficiency and practicability of these strategies are closely related to their atlas. As demonstrated in Table 1, atlases, namely Brodmann, Talairach‑Tournoux, Brain Web, and Whole Brain, are currently in use.

2.2.3 MRF algorithms

The MRF [73] was created to incorporate spatial data into the classification or clustering process. Clustering algorithms minimize the chance of overlapping and the consequences of noise on the conclusion [74]. Conditional Random Fields (CRF) has been proposed as a method of forming
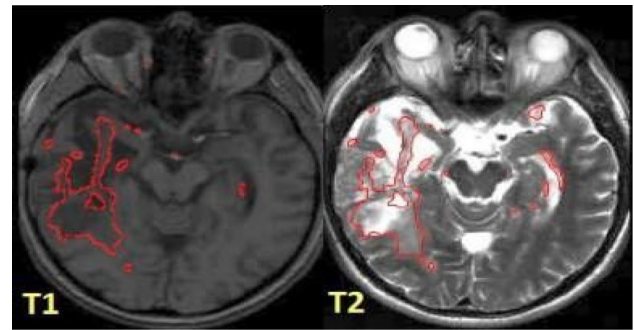

Fig. 3 Fallouts of T1 and T2 brain tumor segmentation

probabilistic representations for segmenting and labeling sequence data [75]. In addition to CRF algorithms, MRF can express complicated connections between datasets to achieve high accuracy in brain tumor segmentation [76]. A Mixture Model (such as GMM) may be used to display several tissues, namely WM, GM, CSF, Active Cells, Necrotic Core, and Edema, and train the MRF using an algorithm called Iterated Condition Modes (ICM) [77]. Each tissue can be segmented easily using various tissue models.

A multi‑layer MRF architecture was devised to detect brain anomalies [78]. The input, geographical location, structural coherence, and region concentrations were the key layers. The multilayer MRF framework projected that a specific voxel's high‑level classification would change if the features of the lower‑level layers were steadily similar in the development of malignancies. Brain tissues were segmented from volumetric MRI brain tumor images using an intuitive technique [83]. This method uses nonrigid registration of a normal atlas in conjunction with the tumor development model to counterfeit soft tissue distortions produced by the effect of a tumor mass. Prior to the registration procedure, the tumor development archetypal, presented as a mesh‑free Markov random field energy reduction issue, guarantees that the atlas and patient image are in sync. Compared to previous methods, this method is non‑parametric and quick while maintaining the same level of accuracy. Using multiwindow Gabor filters and an upgraded MRF framework, a fully

Table 1 Existing Atlas

Name	Depiction	Ref
Brodmann	Primary brain atlas	[79]
Talairach‑ Tournoux	In order to provide standard space, Construct a three‑dimensional Coordinate	[80]
Brain Web	It is usually employed in the examination of MRI brain images	[81]
Whole Brain	At Harvard Medical School, it's used in neurosurgery	[82]

automatic hierarchical probabilistic technique for segmenting tumors from multi-spectral human brain MR images was proposed [84]. The BraTS database was used to divide brain tumors into edema and non-edema groups, as shown in Figure 3. The labels of this algorithm are very similar to those of the experts as shown in Figure 4.

2.2.4 SVM algorithm

Vladimir N. Vapnik devised the Support Vector machine algorithm, and Cortes and Vapnik proposed the existing standard embodiment in 1993 and published it in 1995 [96]. To cope with supervised classification problems, the SVM was handled as a parametrically kernel-based technique [97]. Because of its great classification power, SVM has been extensively applied in the arena of segmenting brain cancer [87–91].

A one-class SVM exploration strategy for the segmentation of brain tumors has been suggested [98]. This technique learned that a nonlinear distribution of image data deprived of past knowledge using an autonomous method of SVM parameter training and an implied learning kernel attained good segmentation fallouts in extracting brain tumors associated with the fuzzy clustering technique. Few researchers have generated voxel-wise intensity-based feature vectors from a large variety of MR image modalities, which have been categorized using SVM [99, 100]. This approach was able to segment not only healthy tissues but also healthy and malignant regions' sub compartments. A similar SVM-based technique was proposed [101], although it discriminated only against one tumor site and utilized fewer modalities.

Subsequently, to improve the findings, feature selection with kernel class separability was included [102]. To extract the tumor from multi-sequence MR images, a multi-kernel-based SVM was suggested, using a feature selection and fusion technique [103]. This method involves two steps: categorizing the tumor area with a multi-kernel SVM algorithm that works on many image bases and produces comparative multi-results, and enhancing the outline of the tumor area with distance and maximum likelihood metrics together. The results of this technique demonstrated a decrease in the overall error and an improvement in accuracy compared to the traditional single-kernel SVM.

Combining SVM classification by multispectral intensities and textures with consequent hierarchical regulation grounded on CRF [104] was expected to provide a completely automatic process for brain tissue segmentation. Figure 5 shows the results of this technique, which uses a tier-up approach to increase the speed by permitting varying quantities of regularization to be applied at different phases to boost robustness and performance. Finally, the SVM showed considerable promise and utility in brain tumor segmentation using Magnetic Resonance images.

As per the methodologies mentioned above, several clustering and classification processes have been utilized to better comprehend the segmentation of MRI-based brain tumors. In recent years, various comparably effective approaches for tumor segmentation using MRI have been developed, as shown in Table 2.

3 Segmentation techniques

This section examines new segmentation approaches and how they have been widely used in digital image-processing applications.

3.1 Deep learning techniques

Deep learning approaches are becoming increasingly popular for image segmentation. These strategies are aimed at obtaining classifier system that is ready to use. The extraction and selection of ROI features are generally used to train the classifier. These processes have proven to be more effective than other machine-learning methods. However, it requires a substantial amount of data as a training data set [85]. As a result, the application of this technique is confined to real-world scenarios because locating large datasets that are generally obtainable is a monotonous task.

A new automatic approach for segmenting liver tumors was proposed by Freiman et al. [86]. The SVM classifier was

Fig. 4 The unlabeled T1C slice, expert labeling, and this algorithm labels are shown from left to right (red- edema, green-non-edema) [84]

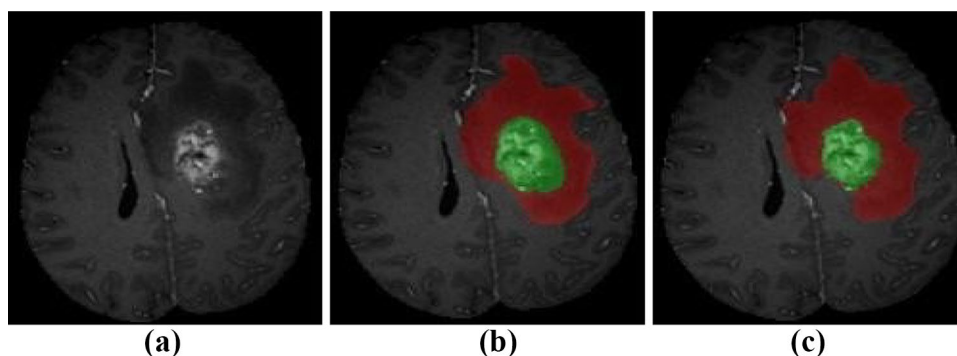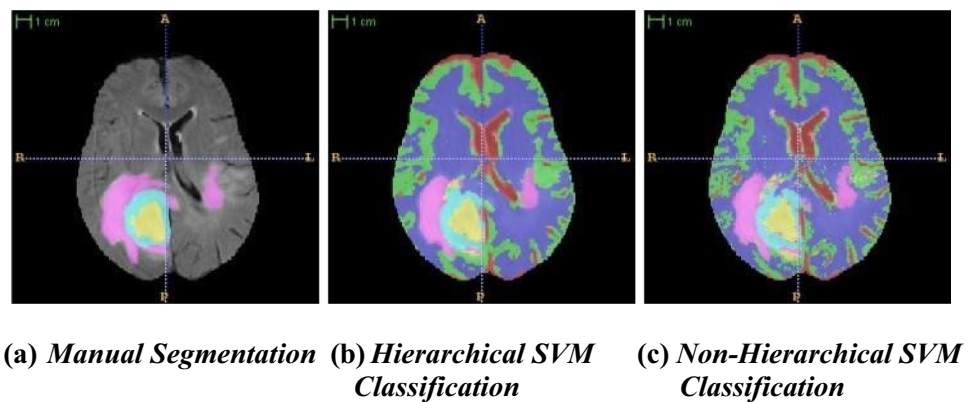**(a)**   **(b)**   **(c)**

Fig. 5 Manual segmentation, hierarchical SVM classification by CRF-regularization, and non-hierarchical SVM classification lacking regularization [93]

(a) *Manual Segmentation*   **(b)** *Hierarchical SVM Classification*   **(c)** *Non-Hierarchical SVM Classification*

utilized to distinguish healthy and cancerous tissues from computer tomography scans, allowing a new batch of high-quality seeds to be created. Compared with many previous semi-automatic procedures, the proposed method is effective and dynamically active. In [87], the authors suggested a fully automatic segmentation system for detecting malignancies in the livers of patients from CT images. The combination of follow-up detection and convolutional neural networks made this method unique (CNN). With automatic feature learning, a CNN was trained to produce a voxel classifier. In terms of accuracy, this method is strong and efficient, with a 60.29 percent improvement over the other methods.

A totally convolutional neural network is anticipated in another study, which results in a more comprehensive ROI segmentation. The following methodology is primarily applicable to biological segmentation issues [88]. With only a few training datasets, the applicability of the model to biomedical segmentation resulted in excellent performance. The strategy is also effective in terms of the amount of time required for training. Christ et al. [89] used a Fully Convolution Neural Network to section the liver and lesions in patients' CT scans

of the abdomen. When related to single fully convolutional networks, the cascaded Fully Convolution Network technique provides better segmentation precision.

3.2 Otsu Thresholding

The Otsu Thresholding segmentation method is a variation of this thresholding approach. Otsu thresholding divides an image into foreground and background classes. The pixels in the image with variable intensity remain repeated on both sides until the interclass variation is minimized. The authors employed this approach in their research [90] to detect and extract brain tumors from MRI data of a patient. Another study used thresholding and morphological techniques to achieve effective and precise identification and segmentation of brain tumors [91].

3.3 FCM with advanced optimization techniques

Fuzzy C Means relies solely on the intensity measurements of pixels and is highly prone to noise. Many researchers

Table 2 MRI-based Brain Tumor Segmentation approaches that are comparably good

Technique	Performance	Reference
Combining k-means with fuzzy c-means	Improved accuracy, reproducibility	[63]
FKSRG	Lowers over-segmentation and under segmentation	[59]
Multi-region and multi-reference outline	Lowers standard deviation and Complex tissue overlap rates	[105]
Combination of Generative probabilistic model and spatial regularization	Compared to typical multivariate tumor segmentation, this is a significant improvement (25 gliomas)	[106]
Probabilistic model in combination with localization	More robust, adapted to display disease development	[72]
Non-rigid registration + atlas + MRF	Multivariate tumor segmentation	[106]
SVM + CRF	Ten multispectral patient datasets, additional detail segmentation with short calculation times	[107]
Decision Forests plus tissue-specific Gaussian mixture models	Different tissue types, like AC, NC, and E, are segmented at the same time	[108]
SVM + Kernel feature selection	Good findings in T1w, T2w, and T1c tests, with a short computation time	[109]

have proposed that spatial relations between pixels should be added to FCM to improve its performance [92]. The updated version of FCM has been shown to improve the segmentation outcomes. Fuzzy C Means (FCM) is a technique for detecting tumor regions in complex MRI data. Preprocessing and image enhancement are performed in the first stage, whereas segmentation and categorization of brain tumors using a learned classifier are performed in the second stage. Several powerful optimization tools have also been applied to diagnose the tumors. Particle Swarm Optimization (PSO) and Genetic Algorithm (GA) are two technologies [93].

Selvakumar et al. [94] projected a framework for determining the range and morphology of brain tumors, as well as their segmentation, by integrating sophisticated K-means and Fuzzy C-means algorithms. Compared with certain manual segmentation procedures, this strategy of integrating the two processes has been demonstrated to be accurate and reproducible. For liver tumor segmentation, Moghbel et al. [95] presented a fully automated technique that required no user interaction. They proposed combining FCM, random walkers' algorithm, and cuckoo search-based optimization in a hybrid approach.

To increase performance in low-contrast images, Fuzzy C-means is a clustering technique that considers each pixel to belong to numerous clusters. A metaheuristic strategy known as cuckoo optimization was used to improve the accuracy of liver segmentation. The random walkers' algorithm, which is based on supervised learning, was used to manage noisy images and fuzzy boundaries in CT scans. From a medical perspective, this model provides accurate tumor segmentation findings and can be integrated into any CAD system for tumor segmentation. A comparison of the various segmentation techniques is presented in Table 3.

4 Deep learning architectures

Deep learning is a subset of a machine-learning algorithm that employs numerous layers to study the order of progressively sophisticated demonstrations from raw data. The goal of machine learning models is to identify appropriate representations of the incoming data. Deep learning has become a popular study topic, and numerous algorithms are available, each with its own set of benefits and downsides. All of these methods enclose virtually every element

Table 3 Comparison of segmentation Techniques

Methodology	Merits	Demerits	New technique proposed
Thresholding	1. Simple to implement	1. Susceptible to noise and grayscale inconsistency.	Otsu Thresholding
	2. cost of computation is low	2. When grayscale values overlap, the results are inaccurate.	
	3. storage space is limited		
	4. Quick processing speed		
Edge detection segmentation	1. Conserves the boundaries of high- contrast images	1. There is a need for manual intervention.	NA
		2. Is unable to detect noise.	
Region based segmentation techniques	1. Implementation is easy	1. Requires manual intervention.	Hemitropic region-growing algorithm
	2. Unaffected by noise	2. Expensive in terms of memory and time to compute.	
Clustering techniques	1. Easy to put into practice	1. Extremely sensitive to noise.	FCM by means of advanced optimization techniques
	2. low computational costs	2. Calculating the membership function is complicated.	
Watershed segmentation	1. Easy to use and understand	1. Excessive segmentation.	Marker Controlled Watershed Segmentation
	2. The algorithm is parallelizable	2. Manual intrusion is required.	
	3. Results in a complete image division	3. Noise sensitive.	
		4. Low contrast boundaries make it difficult to recognize major areas.	
Partial differential Equations	1.Fastest computation	1. Requires precise initialization and implementable functions.	NA
Artificial neural network	1.Less run-time complexity due to a fast segmentation technique	1.Time consumption during the training process.	Deep learning techniques
	2. Excellent sensitivity and accuracy results	2.Works fine with a large Region of Interest.	

of image processing, with a specific prominence in classification and segmentation.

4.1 Classification

Image classification using deep learning is a new development and is a question of success. The most extensively used structure is a convolutional neural network (CNN). Deep learning exploded after Krizhevsky et al. proposed Alex Net, a deep learning archetypal based on a Convolution Neural Network, in 2012 [110], and gained the challenge in ImageNet image categorization during that time. Both VGGNet and Google Net amended the accuracy of the ImageNet dataset in 2014 [111, 112]. The versions of Google Net, such as v2, v3, and v4, have been technologically improved to improve performance [113–115]. He et al. anticipated an enduring ResNet for the model deprivation problem which may emerge as a result of the deep learning model extension, and it has continued to progress deep learning technology [116].

Oxford University's VGG Group was the first to project VGG16. It is similar to Alex Net in that it employs a large number of repeated 3×3 kernels as an alternative to the larger convolution kernels of AlexNet, such as 11×11 and 5×5. Google Net created an inception module for comparison with VGGNet. To reduce the calculation time, it has a solid architecture with a minimal number of convolution kernels of various sizes, and only one convolutional layer.

4.2 Segmentation

Deep learning for semantic segmentation is an important research field. As deep learning technology advances, an increasing number of excellent semantic segmentation neural networks have appeared, and numerous segmentation competitions continue to rank them as state-of-the-art. Others began to experiment with CNN for image segmentation because of their success in classification. Although the Convolution Neural Network can receive images of any size as input, it will miss certain particulars during feature extraction pooling, and it will be unable to locate the spatial information of the original image owing to the entirely linked layers at the network's conclusion. As a result, CNN has trouble determining the group to which certain pixels belong. Some convolutional segmentation networks have become possible owing to advances in deep learning technology.

Long et al. predicted that the fully convolutional network (FCN) [124] will be the creator of semantic segmentation networks. It performs pixel-level classification by replacing the VGG16 classification network's fully connected layers with convolutional layers that retain spatial information of the feature map. Finally, the FCN reestablishes the image by deconvolution and combining feature maps, whereas SoftMax provides pixel segmentation outcomes. Compared with the

Pascal VOC 2012 datasets [125], the performance of the FCN improved by 20% over the previous approach, attaining 62.2 percent of the MIOU.

Based on the FCN, Olaf proposed U-Net [126], which has been extensively utilized in medical tomography. Based on the knowledge of FCN deconvolution, it hypothesizes both encoder and decoder construction to bring back the image size and features. The encoder slowly reduces the spatial measurement, whereas the decoder steadily reinstates the intended spatial dimension based on the element data. The downsampling phase progressively reduces the size of the image, whereas the upsampling phase gradually recovers the image features and size.

Skip connection is a method of directly employing shallow features that differs from traditional convolution, pooling, and other processes. U-Net uses the interweaving skip connection approach to fully utilize the down-sampling characteristics, while also allowing a portion of the encoder to be used for upsampling. This approach was utilized to restrict the feature data of all scales to generate a healthier lessening effect, resulting in a more refined reduction. SegNet [127] is a complicated semantic segmentation network established on an encoder-decoder structure developed by Cambridge to resolve autonomous driving or intelligent robotics. SegNet has 13 convolutional layers in each encoder and decoder. The encoder's convolutional layer corresponds to VGG16's first 13 convolutional layers. The decoder's upsampling section employs unpooling. When the encoder is downsampled, SegNet saves the element location information from the maximum pooling operation and reestablishes the image using this data once sampled on the decoder. SegNet does not involve learning minute upsampling with this method because SegNet training is exact and quicker compared than FCN.

5 Framework for deep learning development

Although deep learning technology has advanced in principle, deep-learning-based software development frameworks are becoming increasingly prevalent. Figure 6 depicts the standard deep-learning network structure.

5.1 Convolution architecture for fast feature embedding (Caffe)

Caffe features rapid speed, easy swapping among Central Processing Unit and Graphics Processing Unit modes, and cross-platform bolster for Windows, Mac, and Linux. The programming framework consists of three major atomic designs: blobs, layers, and nets. It knowingly increases the implementation act through a complicated design and offers affability based on well-organized applications.
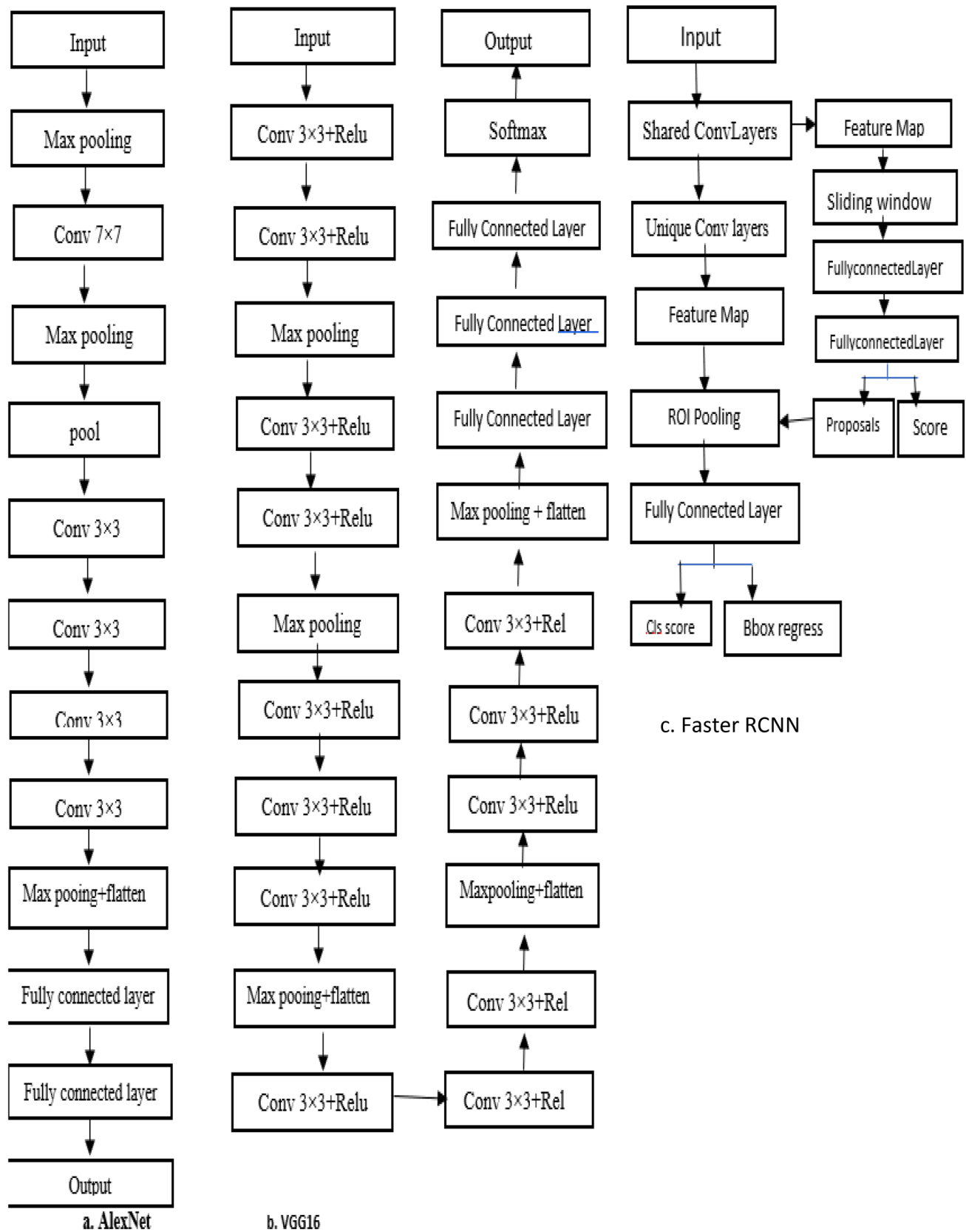
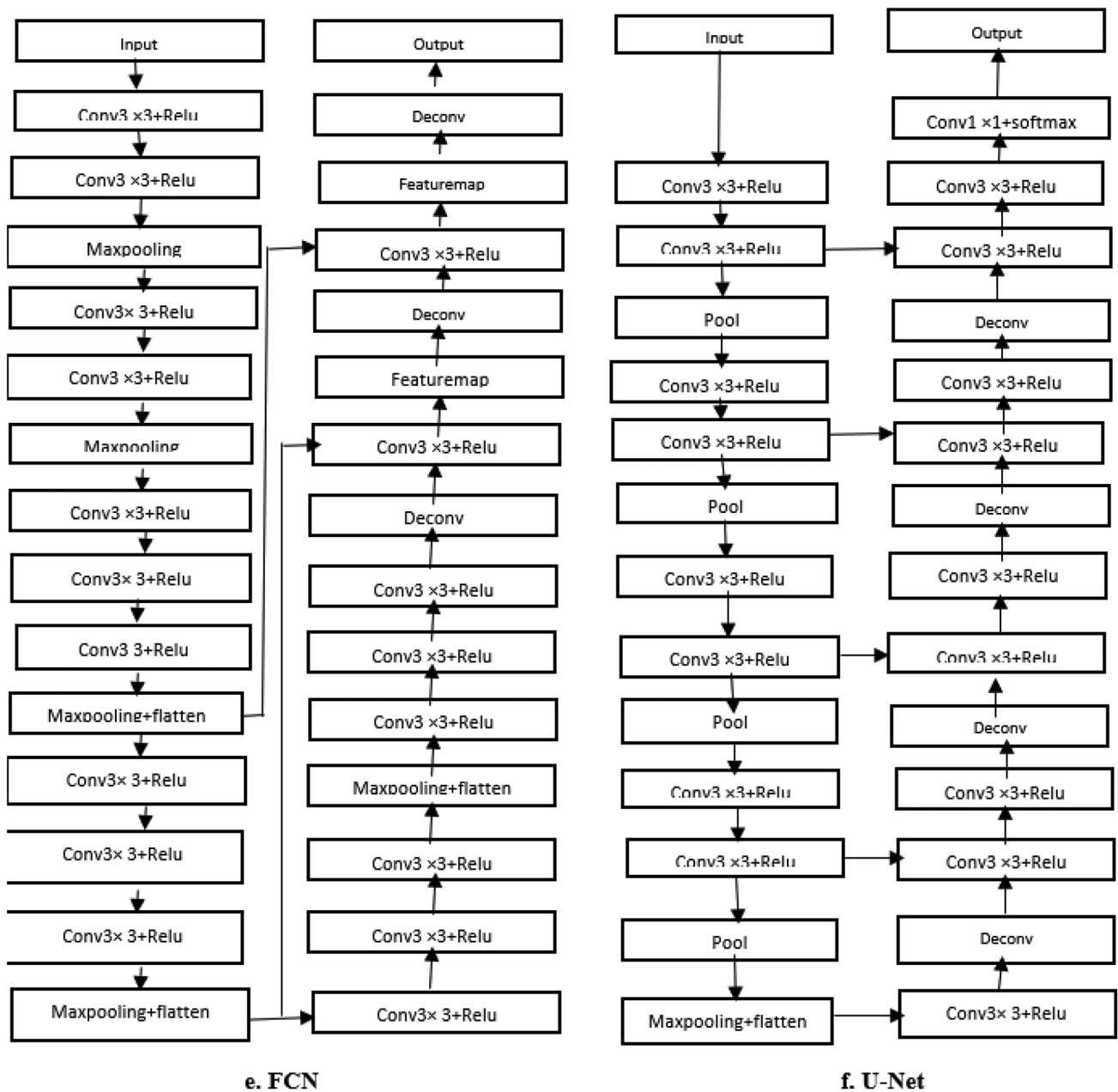**Fig. 6** The standard deep learning network structures

e. FCN

f. U-Net

Fig. 6 (continued)

5.2 TensorFlow

TensorFlow is an open-source framework that uses data-flow diagrams to perform mathematical calculations. Google publicly unveiled the TensorFlow framework on November 9, 2015, and the release of version 1.0 in 2017 signified the framework's formal production deployment. A collection of deep learning algorithms, including RNN, CNN, and LSTM, can be controlled by the TensorFlow calculation framework; however, it can also be applied to standard machine learning. By enabling users to create intricate visual depictions of real-world network topologies and presentations, the Tensor Board significantly expands the visualization capabilities of TensorFlow. Additionally, it supports heterogeneous distributed computing, enabling the model to execute concurrently on several GPUs and various platforms. TensorFlow had a tremendous impact because it was developed in C + + .

5.3 PyTorch

Torch, a neural-network environment designed for GPU-enhanced deep learning, was created using Facebook. PyTorch is the name of Torch in Python. The active Pytorch calculation graph can be modified in real time to satisfy the calculation requirements. It was published on GitHub in January 2017 by the Facebook Artificial Intelligence Institute (FAIR) team, and it was quickly shot to GitHub's hotlist. Soon after its debut, PyTorch attracted considerable attention and quickly gained popularity among scientists.

5.4 High-performance computation based on graphics processing unit

The three most significant components of image processing in medical imaging are picture magnitude, resolution, and imaging speed. Due to technological restrictions, medical image processing is performed sequentially. GPU has made significant advancements in recent years and has begun to move along the route of generic computations. The data-processing capacity of a GPU is significantly greater than that of a CPU, allowing high-performance computing on standard PCs. The graphics processing unit (GPU) is a CPU that performs image computation on PCs, game consoles, workstations, and a few mobile devices. At the time of its creation, it was primarily meant to depict visual pictures. The GPU is a graphics card processor that, like the CPU, conducts composite mathematical and geometrical calculations that are essential for graphic interpretation.

6 Datasets

Multiple publicly accessible resources were used to test computer-aided design systems for brain tumor classification. The Brain Web simulated brain MRI database for healthy and sick brains was provided by the McConnell Brain Imaging Center. The Cancer Imaging Archive has created the Repository of Molecular Brain Neoplasia Data (REMBRANDT), which contains pre-surgical multisequence MR imaging scans of 130 individuals. The Section of Biomedical Image Analysis (SBIA) at the Center of Biomedical Image Computing and Analytics (CBICA) at Pennsylvania University has been added to the Medical Image Computing and Computer-Assisted Intervention (MICCAI) challenge database. The Brain Tumor Segmentation (BraTS) dataset is the name of the dataset.

The Harvard Medical School offers the AANLIB database. Normal MRI is included as well as MRI for disorders such as degenerative, neoplastic, cerebrovascular, and infectious diseases. TCIA provides a Reference Image Database to Evaluate Therapy Response (RIDER). MRI data from

19 patients is included. The School of Biomedical Engineering in China has provided CE MRI data for Glioma, Meningioma, and Pituitary tumors, which includes 3064 T1 weighted images. Table 4 summarizes publicly accessible MRI databases.

7 Literature review

7.1 Brain tumor analysis via state-of-the-art machine learning algorithms

A new method for diagnosing brain tumors was developed based on CNNs and maximum fuzzy entropy segmentation. Solo image super-resolution is used to improve the resolution of MR images. The features were extracted using a pretrained ResNet architecture. 95% of the time, the SVM Binary classification was accurate. When employing edge-adaptive total variation for brain tumor classification, the mean-shift clustering technique is applied for segmentation. A multinomial logistic regression model-based brain tumor classification technique was evaluated with 100% accuracy on the BRATS2017 dataset, which consisted of 48 images. However, larger datasets should be used to test the performance of the structure [128].

Keerthana et al. [129] developed an intellectual technique for early brain cancer identification. Threshold-based segmentation was performed after noise removal and skull stripping. GLCM texture features are given to the SVM to categorize tumors into three groups: normal, benign, and malignant. The GA-SVM classifier performs well with the proposed system. The GA is used for tumor segmentation in a well-organized optimization approach for brain tumor classification. With an accuracy of 91.23 percent, the SVM provided GLCM texture characteristics. Polly et al. introduced a K-means segmentation procedure for HGG and LGG brain tumor categorization. From the wavelet features, PCA was used to select ten relevant features. The SVM algorithm was used to distinguish between the normal and abnormal images. The SVM classifier was again used to categorize LGG and HGG cancers in abnormal images. The proposed process achieved 99% accuracy for 440 images. Noise reduction and MRI smoothing were achieved via skull stripping and Gaussian filtering, respectively. GLCM texture features were extracted after K-means segmentation. The system was evaluated using linear, RBF, and cubic SVM kernels on three datasets: local, AANLIB, and RIDER. The accuracy of the linear kernel using fivefold cross-validation was 98%.

[130] suggested a CAD system based on Otsu thresholding for the detection of brain tumors. To determine the threshold for healthy and unhealthy tissues, a customized Otsu approach was applied to the pre-processed MR image. The feature vector is composed of the shape, LBP, Gabor,

Table 4 Summary of accessible MRI dataset

Dataset Name	Provided by	Image Modalities	MRI Type	URL
Brain Web	McConnell Brain Imaging Centre	T1,T2, proton-density weighted	Normal, Multiple sclerosis	https://brainweb.bic.mni.mcgill.ca/brainweb/
REMBRA NDT	TCIA	Multisequence	Normal, Glioma	https://wiki.cancerimagingarchive.net/display/Public/REMBRANDT
BRATS 2015	MICCAI 2015 challenge	T1,T2weighted,FLA IR	GBM, HGG, LGG	https://www.smir.ch/BRATS/start2015
BRATS 2017	MICCAI 2017 challenge	T1,T2weighted,FLA IR	GBM, HGG, LGG	https://www.med.upenn.edu/sbia/brats2017/data.html
BRATS 2018	MICCAI 2018 challenge	T1,T2weighted,FLA IR	GBM, HGG, LGG	https://www.med.upenn.edu/sbia/brats2018.html
AANLIB	Harvard Medical School	T1,T2weighted	Normal, cerebrovascular, neoplastic, degenerative and infectious diseases	https://www.med.harvard.edu/AANLIB
RIDER	TCIA	T1,T2weighted	Tumour	https://wiki.cancerimagingarchive.net/display/Public/RIDER+NEURO+MRI
CMRI	School of Biomedical Engineering China university	T1 weighted	Glioma, Meningioma, pituitary	https://figshare.com/articles/braintumordataset/1512427

and Zenekamoments features. Owing to the fusion of several features, the recommended approach offers greater accuracy. The RLCP (Run length of centralized pattern) method is used to extract texture features. It has an advantage over other approaches in that it can identify directional biassing in textual patterns and preserve textural quality. With 10 rounds of cross-validation, the Naive Bayes classifier achieved 96% classification accuracy. Kumar S. et al. recommended a wavelet-based hybrid approach for classifying brain MRI tumors. PCA is used to select a meaningful feature set. Using an SVM, classification accuracy of 90% was achieved.

The AdaBoost classifier was used in a study by Minz et al. [132] to categorize brain tumors. Noise-reduction techniques include median filtering and threshold-based segmentation. This method classifies objects based on their textures and GLCM features. Using SVM with an RBF kernel, a brain tumor diagnostic approach based on chicken swarm optimization (CSO) was 99 percent accurate [133]. The CSO optimization method was used to optimize the SVM parameters. Shankar et al. [134] advocated employing texture features in combination with Gustafson-Kessel fuzzy clustering to categorize brain tumors. A histogram-based technique was used to segment the Wiener filter- preprocessed images. The G-K fuzzy approach provides GLCM texture characteristics for binary classification with a 95% accuracy rate. A list of the numerous state-of-the-art strategies is presented in Table 5.

The accuracy of the brain tumor diagnosis using machine learning techniques is shown in Figure 7. The accuracy of the SVM method was higher than that of the other algorithms,

as can be seen from the graph. KNN is ranked second, with 98 percent accuracy, followed by the Naive Bayes algorithm. AdaBoost achieved the lowest accuracy rate, whereas the G-K Fuzzy system displayed a 95% accuracy rate.

## 7.2 Deep learning techniques for detecting brain tumors

A pioneering area of research involves the use of deep learning algorithms to identify brain cancer. Brain tumors are categorized using LinkNet, which is a simple DNN architecture [136]. Binary classification provided 91 percent accuracy on a dataset from the UCI repository that was made publicly available. A brain MRI cancer diagnosis system based on a Deep Wavelet Autoencoder-based Deep Neural Network (DWA-DNN) was proposed by Mallick et al. [137]. The multilayer perceptron (MLP) classifier was 96% accurate with a kappa of 0.65. A sparse autoencoder may still be studied in the future when a DNN is combined with other autoencoder variations such as a denoising autoencoder. Swati et al. [138] advocated the use of transfer learning to categorize brain cancer. To fit the VGG19 model, the MRI scans were scaled to 224x224 pixels. To update the weights, modifications are performed block by block to factors, including the learning rate, scheduling pace, and momentum. The method performed well, with 94.82 percent accuracy on a CE-MRI dataset. The drawback of this strategy is that it requires 20 to 30 minutes to fine-tune settings block by block to train the CNN classifier.

Table 5 ML-based brain tumor detection

Reference	Preprocessing, Segmentation	Features	Classification	Dataset	Accuracy
[117]	Enhancement and resizing of Image	CNN, GLCM	SVM	Local-Iraqi center of research	99.30%
[118]	The morphological process, Segmentation with entropy threshold, pixel subtraction	Morphological, Intensity	Naive Bayes	REMBRANDT	94%
[119]	Super Resolution for a Single Image for Image Enhancement, Maximum fuzzy entropy (MFE) segmentation	Deep features of ResNet	SVM	TCIA	95%
[120]	normalization using min–max, Resize 224*224	Deep features on Google Net	KNN, SVM	CE-MRI	SVM- 97.8% KNN- 98%
[121]	Median filtering, GA segmentation	GLCM	SVM	Harvard Medical Dataset	91.23%
[122]	OTSU Binarization and K-means clustering	DWT	SVM	BRATS 2013, BRATS 2017, Midas	99%
[123]	Skull stripping using BSE Gaussian filter, segmentation using k-Means	GLCM, Intensity, shape	SVM	Local, AANLIB, and RIDER	98%
[124]	Image enhancement-DSR-AD, segmentation using the OTSU method	Tamura, GLCM, Gabor, Shape, LBP	SVM	Local	98%
[125]	Enhancement by means of DSR- AD, Adaptive global segmentation	RLCP	Naive Bayes	Local-JMCD, BRATS	96%
[126]	A median filter for noise removal, Threshold-based segmentation	GLCM	Adaboost	Public dataset	89.90%
[127]	Wiener filtering, Histogram based segmentation	Gray-Level Co-Occurrence Matrix	Gustafson-Kessel Fuzzy clustering	-	95%

MLP is a statistical and wavelet-based classification system for brain malignancies [139]. Both the statistical and DWT characteristics, as well as a merged feature set, were used to evaluate the system. The combined feature set performed well, with a precision of 96.73 percent. The system demonstrates classification robustness for a large dataset of 40,300 images. Non-sub-sampled contour transform is an enhancement method used to detect glioma tumors with ANFIS classification [140]. ANFIS was used to classify brain tumor types into normal and glioma, using the BRATS 2015 dataset. For low-intensity Glioma images, traditional classification algorithms such as SVM and CNN

Fig. 7 Accuracy of Brain Tumor detection using ML Algorithms
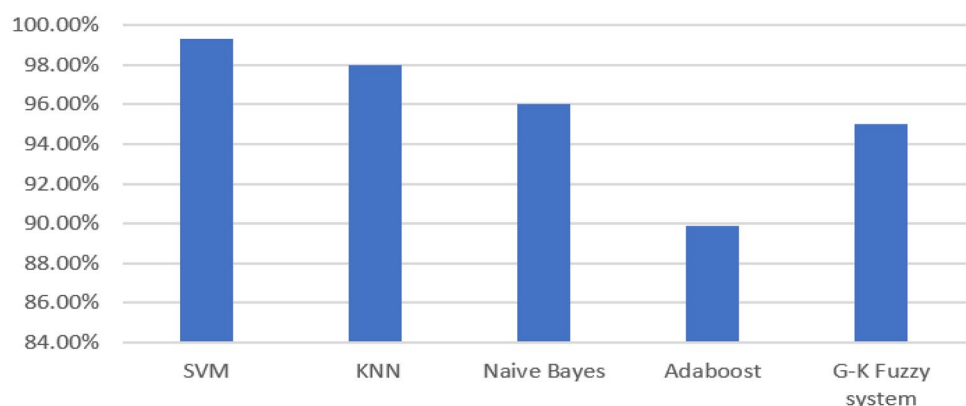
create classification errors, ANFIS, on the other hand, is effective for both low and high-intensity Gliomas. A seven-layer DNN architecture was used to categorize the tumor types into four classes: normal, sarcoma, carcinoma, and glioblastoma [141]. In the future, a CNN-based CAD system for brain tumor grade classification may be developed to improve the performance.

Based on MRI data, [142] suggested grading brain tumors using CNN and GA. Glioma, meningioma, and pituitary malignancies can be classified using a CNN with five convolutional layers and two fully linked layers. A CNN with six convolutional layers and two fully linked layers was used to categorize gliomas. The number of convolution layers, maximum number of pooling layers, number of filters, size of the filters, activation function, and learning rate are the CNN parameters that GA chooses. For the BRATS dataset, 10 fuzzy rules were used to assess a novel method for classifying brain tumors using the neuro-fuzzy feature selection process [143]. An effective method for distinguishing between high- and low-grade tumors is an Adaptive Neuro-Fuzzy Classifier (ANFC). Lavanyadev et al. [144] proposed a novel PNN-based approach for brain tumor classification. K-indicates that GLCM texture features occur after segmentation. Colored MRI scans were used to extract three-color moments: mean, standard deviation, and skewness [145]. Table 3 provides a summary of various deep Learning approaches.

8 Analysis

The segmentation of tumors in the brain is crucial and is normally performed by a professional radiologist who uses machine learning and deep learning methods to make decisions. This study provides an overview of several sophisticated strategies for automatically detecting brain tumors. To preprocess MRI images, processes such as median, Gaussian, Wiener filter, histogram measurement, and skull removal are utilized. There are six classification approaches: combination methods, mathematics, ANN, regional-based edge-finding methods, and edge-finding methods. Researchers frequently utilize C-combining, dynamic, and global approaches owing to their fuzzy K-means.

The most extensively used feature extraction tools are the GLCM and DWT. GLCM provides standing features, whereas DWT receives measurement coefficients as feature vectors. A multidisciplinary approach is employed for effective classification because identifying the optimal attributes for the correct categorization is difficult. CNN has shown good segmentation results when used with transfer learning models, such as VGG19 and Res Net. ANFIS, which combines a mysterious system with an artificial neural network, is divided into two sections. BRAT is a common dataset comprising T1-weighted, T2-weighted, and FLAIR images. However, one database did not include all types of cancer

Table 6 Summary of DL-based Brain Tumor detection

Ref	Pre-processing	Classification	Dataset	Accuracy
[128]	Intensity normalization, contrast enhancement	RELM	CE-MRI	94.33%
[129]	Average filter, Pixel subtraction	CNN-Link Net	UCI	91%
[130]	DICOM image processing, DWT-DNN features	MLP	RIDER	96%
[131]	Min–Max intensity normalization	VGG-19	CE-MRI	94.82%
[132]	Histogram, GLCM, DWT features	MLP	BRATS 2015	96.73%
[133]	NSCT image enhancement, GLCM texture features	ANFIS	BRATS 2015	98.5%
[134]	DWT features	DNN	AANLIB	96.97%
[135]	segmentation based on Bayesian Fuzzy clustering, information theoretic, scatters and wavelet features	HSC based multi SVNN	BRATS	93%
[136]	smoothing and Sharpening filters, Threshold-based segmentation, SGLD features	ANN	AANLIB	99%
[137]	Input cascade CNN segmentation, data augmentation	VGG 19	CE-MRI	94.58%
[138]	Image rescaling, data augmentation	CNN	Brain web, REMBRANDT, CE-MRI	96%
[139]	VOI segmentation, GLCM, GLS, GLRL, GSS features	ANFH-LS	BRATS 2012, BRATS 2013	85.83%
[141]	Median filter, color moments, feature extraction	ANN	AANLIB	95%

Fig. 8 Accuracy of Brain Tumor detection using DL Algorithms
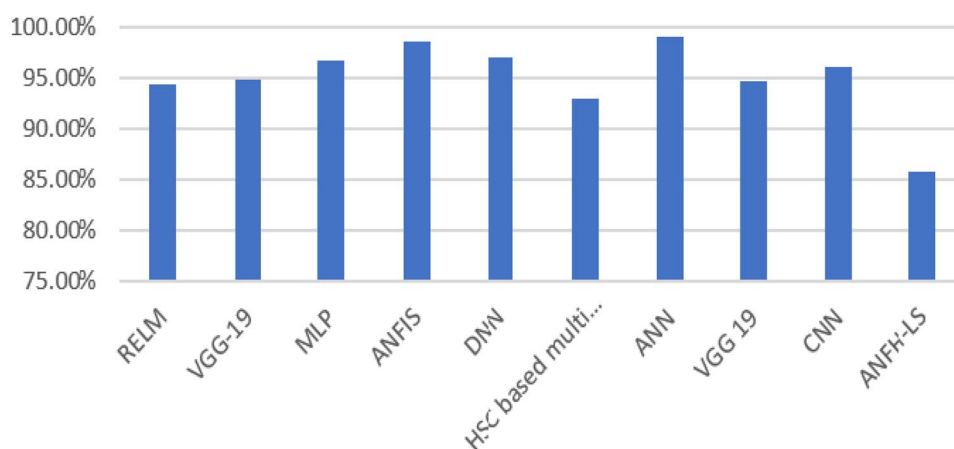
and the distances involved. Table 6 provides a review of brain tumor detection using deep learning.

Figure 8 illustrates the effectiveness of deep learning systems in detecting brain cancer. The graph shows that the ANN outperforms all other algorithms with 99% accuracy, followed by ANFIS with 98.5 percent accuracy, and DNN and MLP with approximately the same accuracy rate of 96%. The accuracy of the CNN was 96%, and the VGG-19 and RELM were almost as accurate at 94.58% and 94.33%, respectively. The HSC-based multi-SVNN was next with 93% accuracy, and the ANFH-LS achieved an accuracy of 85.83%.

9 Conclusion

As there has been a considerable increase in brain tumor cases in recent years, scientists and researchers working in related fields have found that it motivates the development of effective methods for identifying brain tumors. The objective of this review is to increase scholars' interest in this difficult field and to familiarize them with current advancements. Digital image processing approaches, such as preprocessing, segmentation, and classification are applied to create CAD systems aimed at brain tumor identification using MR images. Classic machine learning and deep learning approaches for brain tumor identification are discussed in this work. This paper provides a summary of commonly used MR image datasets. For classification, various machine learning and deep learning algorithms have been acclimated, yet SVM has been shown to be accurate. The SVM is often used to categorize brain tumors into two types: normal and pathological. The development of an autonomous brain tumor detection system must consider reliability, accuracy, and calculation time. This survey examines current methodologies and can be utilized in the future to develop effective diagnostic plans for other brain disorders such as dementia, Alzheimer's disease, stroke, and Parkinson's disease using various Magnetic Resonance imaging modalities.

Declarations

References

1. DeAngelis LM. Brain Tumors. N Engl J Med. 2001;344(2):114–23.
2. Louis DN, et al. The 2016 World Health Organization classification of tumors of the central nervous system: a summary. Acta Neuropathol (Berl). 2016;131(6):803–20.
3. Birry RAK. Automated Classification in Digital Images of Osteogenic Differentiated Stem Cells. Ph.D. Thesis, University of Salford, Salford, UK, 2013.
4. Liu J, Li M, Wang J, Wu F, Liu T, Pan Y. A survey of MRI-based brain tumor segmentation methods. Tsinghua Sci Technol. 2014;19(6):578–595. View at: Publisher Site | Google Scholar | MathSciNet.
5. Bauer S, Wiest R, Nolte LP, & Reyes M. A survey of MRI based medical image analysis for brain tumor studies. Phys Med Bio. 2013;58(13):97–129. View at: Google Scholar.
6. Helms G, Kallenberg K, Dechent P. Contrast-driven approach to intracranial segmentation using a combination of T2- and T1- weighted 3D MRI data sets. J Magn Reson Imaging 2006;24(4):790–795. View at: Publisher Site | Google Scholar.
7. Gibbs P, Buckley D, Blackb S, Horsman A. Tumour determination from MR images by morphological segmentation. Phys Med Biol. 1996;41(11):2437–46.
8. Stadlbauer A, Moser E, Gruber S, et al. Improved delineation of brain tumors: An automated method for segmentation based on pathologic changes of 1H-MRSI metabolites in gliomas. Neuroimage. 2004;23(2):454–61.
9. Kaus MR, Warfeld SK, Nabavi A, Black PM, Jolesz FA, Kikinis R. Automated segmentation of MR images of brain tumors. Radiology. 2001;218(2):586–91.
10. Deng W, Xiao W, Deng H, Liu J. MRI brain tumor segmentation with region growing method based on the gradients and

      variances along and inside of the boundary curve. in Proceedings of the 3rd International Conference on BioMedical Engineering and Informatics, BMEI 2010; 393–396, China, October 2010.

11. Taheri S, Ong SH, Chong VFH. Level-set segmentation of brain tumors using a threshold-based speed function. Image Vis Comput. 2010;28(1):26–37.

12. Sachdeva J, Kumar V, Gupta I, Khandelwal N, Ahuja CK. A novel content-based active contour model for brain tumor segmentation. Magn Reson Imaging. 2012;30(5):694–715.

13. Wang T, Cheng I, Basu A. Fluid vector flow and applications in brain tumor segmentation. IEEE Trans Biomed Eng. 2009;56(3):781–9.

14. Hasan AM, Meziane F, Aspin R, Jalab HA. Segmentation of brain tumors in MRI images using three-dimensional active contour without edge. Symmetry 2016;8(11):132.

15. Fletcher-Heath LM, Hall LO, Goldgof DB, Murtagh FR. Automatic segmentation of non-enhancing brain tumors in magnetic resonance images. Artif Intell Med. 2001;21(1–3):43–63.

16. Veloz A, Chabert S, Salas R, Orellana A, Vielma J. Fuzzy spatial growing for glioblastoma multiforme segmentation on brain magnetic resonance imaging. LNCS. 2008;4756:861–70.

17. Havaei M, Davy A, Warde-Farley D, et al. Brain tumor segmentation with Deep Neural Networks. Med Image Anal. 2017;35:18–31.

18. Pereira S, Pinto A, Alves V, Silva CA. Brain Tumor Segmentation Using Convolutional Neural Networks in MRI Images. IEEE Trans Med Imaging. 2016;35(5):1240–51.

19. Isin A, Direkoglu C, Sah M. Review of MRI-based brain tumor image segmentation using deep learning methods. Procedia Comput Sci. 2016;102:317–24.

20. Gordillo N, Montseny E, Sobrevilla P. State of the art survey on MRI brain tumor segmentation. Magn Reson Imaging. 2013;31(8):1426–38.

21. Ortiz A, Gorriz JM, Ramirez J, Salas-Gonzalez D. Improving MR brain image segmentation using self-organizing maps and entropy-gradient clustering. Inform Sci. 2014;262:117–36.

22. White D, Houston A, Sampson W, Wilkins G. Intra and interoperator variations in region-of-interest drawing and their effect on the measurement of glomerular filtration rates. 1999;24:177–81.

23. Foo JL. A survey of user interaction and automation in medical image segmentation methods. Tech rep ISUHCI20062, Human Computer Interaction Department, Iowa State Univ. 2006.

24. Hamamci A, et al. Tumor-Cut: segmentation of brain tumors on contrast enhanced MR images for radiosurgery applications. IEEE Trans Med Imaging. 2012;31(3):790–804.

25. Havaei M, Larochelle H, Poulin P, Jadoin PM. Within-brain classification for brain tumor segmentation. Int J Cars. 2016;11:777–88.

26. Suzuki H, Toriwaki J-I. Automatic segmentation of head MRI images by knowledge guided thresholding. Comput Med Imaging Graph. 1991;15(4):233–40.

27. Harris G, Barta P, Peng L, Lee S, Brettschneider P, Shah A, Henderer J, Schlaepfer T, Pearlson G. MR volume segmentation of gray matter and white matter using manual thresholding: Dependence on image brightness. Am J Neuroradiol. 1994;15(2):225–30.

28. Adams R, Bischof L. Seeded region growing. Pattern Analysis and Machine Intelligence, IEEE Transactions on. 1994;16(6):641–7.

29. Vijayakumar C, Gharpure DC. Development of image-processing software for automatic segmentation of brain tumors in MR images. J Med Phys Assoc Med Phys India. 2011;36(3):147.

30. Wong K-P. Medical image segmentation: Methods and applications in functional imaging, in Handbook of Biomedical Image Analysis. Springer. 2005;111–182.

31. Mittelhaeusser G, Kruggel F. Fast segmentation of brain magnetic resonance tomograms, in Computer Vision, Virtual Reality and Robotics in Medicine. Springer. 1995;237–241.

32. Kaus MR, Warfield SK, Nabavi A, Black PM, Jolesz FA, Kikinis R. Automated segmentation of MR images of brain tumors 1. Radiology. 2001;218(2):586–91.

33. Chong VF, Zhou J-Y, Khoo JB, Huang J, Lim T-K. Tongue carcinoma: Tumor volume measurement. Int J Radiat Oncol Biol Phys. 2004;59(1):59–66.

34. Salman Y, Assal M, Badawi A, Alian S, El-Bayome ME. Validation techniques for quantitative brain tumors measurements, in Engineering in Medicine and Biology Society. IEEE-EMBS 2005. 27th Annual International Conference of the. IEEE. 2005;2006:7048–51.

35. Sato M, Lakare S, Wan M, Kaufman A, Nakajima M. A gradient magnitude based region growing algorithm for accurate segmentation, in Image Processing, 2000. Proceedings. 2000 International Conference on, IEEE, 2000;3:448–451.

36. Lakare S, Kaufman A. 3D segmentation techniques for medical volumes. Center for Visual Computing: Department of Computer Science, State University of New York; 2000.

37. Salman YM. Modified technique for volumetric brain tumor measurements. J Biomed Sci Eng. 2009;2:16.

38. Dou W, Ruan S, Chen Y, Bloyet D, Constans J-M. A framework of fuzzy information fusion for the segmentation of brain tumor tissues on MR images. Image Vis Comput. 2007;25(2):164–71.

39. Letteboer M, Niessen W, Willems P, Dam EB, Viergever M. Interactive multi-scale watershed segmentation of tumors in MR brain images, in Proc. of the IMIVA Workshop of MICCAI, Citeseer. 2001.

40. Dam E, Loog M, Letteboer M. Integrating automatic and interactive brain tumor segmentation, in Pattern Recognition, 2004. ICPR 2004. Proceedings of the 17th International Conference on, IEEE. 2004(3):790–793.

41. Cates JE, Whitaker RT, Jones GM. Case study: An evaluation of user-assisted hierarchical watershed segmentation. Med Image Anal. 2005;9(6):566–78.

42. Ratan R, Sharma S, Sharma S. Multiparameter segmentation and quantization of brain tumor from MRI images. Indian J Sci Technol. 2009;2(2):11–5.

43. Salman SD, Bahrani AA. Segmentation of tumor tissue in gray medical images using watershed transformation methods. International Journal of Advancements in Computing Technology. 2010;2(4):123–7.

44. Bleau A, Leon LJ. Watershed-based segmentation and region merging. Comput Vis Image Underst. 2000;77(3):317–70.

45. Gies V, Bernard TM. Statistical solution to watershed over-segmentation. In Int Conf Image Proc. 2004.

46. Kong J, Wang J, Lu Y, Zhang J, Li Y, Zhang B, A novel approach for segmentation of MRI brain images, in Electrotechnical Conference,. MELECON 2006. IEEE Mediterranean, IEEE. 2006;2006:525–8.

47. Duda RO, Hart PE, Stork DG. Pattern Classification. John Wiley & Sons. 2012.

48. Bishop CM. Pattern Recognition and Machine Learning, vol. 1. New York: Springer; 2006.

49. Mitchell TM. The discipline of machine learning. School of Computer Science: Carnegie Mellon University; 2006.

50. Alpaydin E. Introduction to Machine Learning. MIT Press. 2004.

51. Hastie T, Tibshirani R, Friedman J, Franklin J. The elements of statistical learning: Data mining, inference, and prediction. The Mathematical Intelligencer. 2005;27(2):83–5.

52. Chapelle O, Scholkopf B, Zien A. (ed.) SemiSupervised Learning, vol. 2. MIT Press Cambridge. 2006.

53. Christakou C, Lefakis L, Vrettos S, Stafylopatis A. A movie recommender system based on semi-supervised clustering, in Computational Intelligence for Modelling, Control and Automation, 2005 and International Conference on Intelligent

Agents, Web Technologies and Internet Commerce. Int Conf IEEE. 2005;(2):897–903.

54. Bezdek JC. Pattern Recognition with Fuzzy Objective Function Algorithms. Kluwer Academic Publishers. 1981.

55. Hall LO, Bensaid AM, Clarke LP, Velthuizen RP, Silbiger MS, Bezdek JC. A comparison of neural network and fuzzy clustering techniques in segmenting magnetic resonance images of the brain. Neural Networks, IEEE Transactions on. 1992;3(5):672–82.

56. Phillips W II, Velthuizen R, Phuphanich S, Hall L, Clarke L, Silbiger M. Application of fuzzy c means segmentation technique for tissue differentiation in mr images of a hemorrhagic glioblastoma multiforme. Magn Reson Imaging. 1995;13(2):277–90.

57. Clark MC, Hall LO, Goldgof DB, Velthuizen R, Murtagh FR, Silbiger MS. Automatic tumor segmentation using knowledge-based techniques. Medical Imaging, IEEE Transactions on. 1998;17(2):187–201.

58. Fletcher-Heath LM, Hall LO, Goldgof DB, Murtagh FR. Automatic segmentation of non-enhancing brain tumors in magnetic resonance images. Artif Intell Med. 2001;21(1):43–63.

59. Lin G-C, Wang W-J, Kang C-C, Wang C-M. Multispectral MR images segmentation based on fuzzy knowledge and modified seeded region growing. Magn Reson Imaging. 2012;30(2):230–46.

60. Szilagyi L, Benyo Z, Szilagyi SM, Adam H. MR brain image segmentation using an enhanced fuzzy C means algorithm, in Engineering in Medicine and Biology Society, 2003. Proceedings of the 25th Ann Int Conf IEEE, IEEE. 2003;1:724–726.

61. Cai W, Chen S, Zhang D. Fast and robust fuzzy c-means clustering algorithms incorporating local information for image segmentation. Pattern Recogn. 2007;40(3):825–38.

62. Forouzanfar M, Forghani N, Teshnehlab M. Parameter optimization of improved fuzzy c-means clustering algorithm for brain MR image segmentation. Eng Appl Artif Intell. 2010;23(2):160–8.

63. Gupta MP, Shringirishi MM. Implementation of brain tumor segmentation in brain MR images using k-means clustering and fuzzy c-means algorithm. Int J Comput Technol. 2013;5(1):54–9.

64. Maintz J, Viergever MA. A survey of medical image registration. Med Image Anal. 1998;2(1):1–36.

65. Cuadra MB, Pollo C, Bardera A, Cuisenaire O, Villemure J-G, Thiran J. Atlas-based segmentation of pathological MR brain images using a model of lesion growth, Medical Imaging, IEEE Transactions 2004;23(10):1301–1314.

66. Dempster P, Laird NM, Rubin DB. Maximum likelihood from incomplete data via the em algorithm. J Roy Stat Soc. 1977;39(1):1–38.

67. Moon N, Bullitt E, Van Leemput K, Gerig G. Automatic brain and tumor segmentation, in Medical Image Computing and Computer-Assisted Intervention—MICCAI. Springer. 2002;2002:372–9.

68. Prastawa M, Bullitt E, Moon N, Van Leemput K, Gerig G. Automatic brain tumor segmentation by subject specific modification of atlas priors. Acad Radiol. 2003;10(12):1341–8.

69. Mohamed A, Shen D, Davatzikos C. Deformable registration of brain tumor images via a statistical model of tumor-induced deformation, in Medical Image Computing and Computer-Assisted Intervention-MICCAI. Springer. 2005;2005:263–70.

70. Liu T, Shen D, Davatzikos C. Deformable registration of tumor-diseased brain images, in Medical Image Computing and Computer-Assisted Intervention-MICCAI. Springer. 2004;2004:720–8.

71. Cabezas M, Oliver A, Llado X, Freixenet J, Bach Cuadra M. A review of atlas-based segmentation for magnetic resonance brain images. Comput Methods Programs Biomed. 2011;104(3):e158-e177, 2011.

72. Weizman L, Ben Sira L, Joskowicz L, Constantini S, Precel R, Shofty B, Ben Bashat D. Automatic segmentation, internal classification, and follow-up of optic pathway gliomas in mri. Med Image Analys 2012;16(1):177–188.

73. Kindermann R, Snell JL. Markov Random Fields and Their Applications, vol. 1. RI: American Mathematical Society Providence; 1980.

74. Tran TN, Wehrens R, Buydens L. Clustering multispectral images: A tutorial. Chemom Intell Lab Syst. 2005;77(1):3–17.

75. Lafferty J, McCallum A, Pereira FC. Conditional random fields: Probabilistic models for segmenting and labeling sequence data. In Proceedings of the 18th Int Conf Mach Learn. 2001 (ICML 2001).

76. Ekin A, Pathology-robust MR, intensity normalization with global and local constraints, in Biomedical Imaging: From Nano to Macro,. IEEE International Symposium on. IEEE. 2011;2011:333–6.

77. Capelle A-S, Alata O, Fernandez C, Lefevre S, Ferrie J. Unsupervised segmentation for automatic detection of brain tumors in MRI, in Image Processing, 2000. Proceedings. 2000 Int Conf IEEE. 2000;1:613–616.

78. Gering DT, Grimson WEL. and R. Kikinis Recognizing Deviations from Normalcy for Brain Tumor Segmentation: Springer; 2002.

79. Brodmann K. Vergleichende Lokalisationslehre der Gro hirnrinde. Springer. 1909.

80. Talairach J, Tournoux P. Co-Planar Stereotaxic Atlas of the Human Brain: 3-dimensional proportion System— An Approach to Cerebral Imaging. New York, USA: Thieme Medical Publishers; 1988.

81. Evans A, Marrett S, Torrescorzo J, Ku S, Collins L. Mri-pet correlation in three dimensions using a volume of interest (voi) atlas. J Cereb Blood Flow Metab. 1991;11:A69–78.

82. Shenton M, Kikinis R, McCarley W, Saviiroonporn P, Hokama H, Robatino A, Metcalf D, Wible C, Portas C, Iosifescu D et al. Harvard brain atlas: A teaching and visualization tool. In Proceedings of the 1995 Biomed Visualization. 1995;10–17.

83. Bauer S, Nolte L-P, Reyes M, Segmentation of brain tumor images based on atlas-registration combined with a Markov-random- field lesion growth model, in Biomedical Imaging: From Nano to Macro,. IEEE International Symposium on. IEEE. 2011;2011:2018–21.

84. Subbanna NK, Precup D, Collins DL, Arbel T. Hierarchical probabilistic gabor and MRI segmentation of brain tumours in mri volumes, in Medical Image Computing and Computer-Assisted Intervention-MICCAI. Springer. 2013;2013:751–8.

85. Kuo CL, Cheng SC, Lin CL, Hsiao KF, Lee SH. Texture-based Treatment Prediction by Automatic Liver Tumor Segmentation on Computed Tomography. IEEE. 2017.

86. Freiman M, Cooper O, Lischinski D, Joskowicz L. Liver tumors segmentation from CTA images using voxels classification and affinity constraint propagation. Int J Comput Assist Radiol Surg. 2011;6:247–55.

87. Vivanti R, Ephrat A, Joskowicz L, Karaasla OA, Lev-Cohain N, Sosna J. Automatic liver tumor segmentation in follow-up CT studies using Convolutional Neural Networks. In: International Workshop on Patch-based Techniques in Medical Imaging, Springer; 2015. pp. 54–61.

88. Ronneberger O, Fischer P, Brox T. U-net: Convolutional networks for biomedical image segmentation," in: MICCAI. 2015;9351:234–241.

89. Christ PF, Elshaer MEA, Ettlinger F, Tatavarty S, Bickel M, Bilic P, Rempfler M, Armbruster M, Hofmann F, D'Anastasi M, Sommer WH, Ahmadi S-A, Menze BH. Automatic liver and lesion segmentation in CT using cascaded fully convolutional

neural networks and 3D conditional random fields," MICCAI, Cham; 2016. pp. 415–423.

90. Rajesh C. Patil, Dr. A. S. Bhalchandra, "Brain Tumor Extraction from MRI Images Using MATLAB" International Journal of Electronics, Communication & Soft Computing Science and Engineering ISSN: 2277–9477, vol. 2, no. 1, April 2012.

91. Murthy TSD, Sadashivappa G. Brain tumor segmentation using thresholding, morphological operations and extraction of features of tumor. 2014 Int Conf Adv Electron Comput Commun; 2014.

92. Kapoor L, Thakur S. A Survey on Brain Tumor Detection Using Image Processing Techniques. 2017 7th International Conference on Cloud Computing, Data Science & Engineering – Confluence, IEEE; 2017. pg. 582–585.

93. Gopal NN, Karnan M. Diagnose brain tumor through MRI using image processing clustering algorithms such as Fuzzy C Means along with intelligent optimization techniques. 2010 IEEE Int Conf Comput Intell Comput Res. 2010.

94. Sivakumar J, Lakshmi A, Arivoli T. Brain Tumor Segmentation and Its Area Calculation in Brain MR Images using K-Mean Clustering and Fuzzy C-Mean Algorithm. 2012 IEEE- Int Conf Adv Eng Sci Manag (ICAESM 2012); 2012.

95. Moghbel M, Mashohor S, Mahmud R, Iqbal Bin Saripan M. Automatic liver tumor segmentation on computed tomography for patient treatment planning and monitoring. EXCLI J. 2016;15:406–423.

96. Cortes C, Vapnik V. Support-vector networks. Mach Learn. 1995;20(3):273–97.

97. Vapnik V. The Nature of Statistical Learning Theory. Springer; 2000.

98. J. Zhou, K. Chan, V. Chong, S. Krishnan, Extraction of brain tumor from mr images using one-class support vector machine, in Engineering in Medicine and Biology Society. IEEE-EMBS 2005. 27th Annual International Conference of the. IEEE. 2005;2006:6411–4.

99. Cai H, Verma R, Ou Y, Lee S-K, Melhem ER, Davatzikos C, Probabilistic segmentation of brain tumors based on multi- modality magnetic resonance images, in Biomedical Imaging: From Nano to Macro,. ISBI 2007. 4th IEEE International Symposium on. IEEE. 2007;2007:600–3.

100. Verma R, Zacharaki EI, Ou Y, Cai H, Chawla S, Lee S-K, Melhem ER, Wolf R, Davatzikos C. Multiparametric tissue characterization of brain neoplasms and their recurrence using pattern classification of mr images. Acad Radiol. 2008;15(8):966–77.

101. Ruan S, Lebonvallet S, Merabet A, Constans J, Tumor segmentation from a multispectral mri images by using support vector machine classification, in Biomedical Imaging: From Nano to Macro,. ISBI 2007. 4th IEEE International Symposium on. IEEE. 2007;2007:1236–9.

102. Ruan S, Zhang N, Liao Q, Zhu Y, Image fusion for following-up brain tumor evolution, in Biomedical Imaging: From Nano to Macro,. IEEE International Symposium on. IEEE. 2011;2011:281–4.

103. Zhang N, Ruan S, Lebonvallet S, Liao Q, Zhu Y. Multi-kernel SVM based classification for brain tumor segmentation of MRI multi-sequence, in Image Processing (ICIP). 2009 16th IEEE Int Conf IEEE; 2009, pp. 3373–3376.

104. Bauer S, Nolte L-P, Reyes M. Fully automatic segmentation of brain tumor images using support vector machine classification in combination with hierarchical conditional random field regularization, in Medical Image Computing and Computer-Assisted Intervention-MICCAI. Springer. 2011;2011:354–61.

105. Shi F, Yap P-T, Fan Y, Gilmore JH, Lin W, Shen D. Construction of multi-region-multi-reference atlases for neonatal Brain MRI segmentation. Neuroimage. 2010;51(2):684–93.

106. Menze BH, Van Leemput K, Lashkari D, Weber M-A, Ayache N, Golland P. A generative model for brain tumor segmentation in multi-modal images, in Medical Image Computing and Computer-Assisted Intervention- MICCAI. Springer. 2010;2010:151–9.

107. Bauer S, Nolte L-P, Reyes M. Fully automatic segmentation of brain tumor images using support vector machine classificatio in combination with hierarchical conditional random field regularization, in Medical Image Computing and Computer-Assisted Intervention-MICCAI. Springer. 2011;2011:354–61.

108. Zikic D, Glocker B, Konukoglu E, Criminisi A, Demiralp C, Shotton J, Thomas O, Das T, Jena R, Price S. Decision forests for tissue-specific segmentation of high-grade gliomas in multi-channel MR, in Medical Image Computing and Computer-Assisted Intervention- MICCAI. Springer. 2012;2012:369–76.

109. Zhang N, Ruan S, Lebonvallet S, Liao Q, Zhu Y. Kernel feature selection to fuse multi-spectral MRI images for brain tumor segmentation. Comput Vis Image Underst. 2011;115(2):256–69.

110. Krizhevsky A, Sutskever I, Hinton GE. Imagenet classification with deep convolutional neural networks. In: Adv Neural Inf Proces Syst. 2012:1097–105.

111. Szegedy C, Liu W, Jia Y, et al. Going deeper with convolutions. In: Proceedings of the IEEE Conf Comput Vis Pat Recog. 2015:1–9.

112. Simonyan K, Zisserman A. Very deep convolutional networks for large-scale image recognition. 2014. arXiv preprint arXiv:1409.1556.

113. Ioffe S, Szegedy C. Batch normalization: accelerating deep network training by reducing internal covariate shift. 2015. arXiv preprint arXiv:1502.03167.

114. Szegedy C, Vanhoucke V, Ioffe S, et al. Rethinking the inception architecture for computer vision. In: Proceedings of the IEEE Conf Comput Vis Pat Recog. 2016:2818–26.

115. Szegedy C, Ioffe S, Vanhoucke V, et al. Inception-v4, inception-resnet and the impact of residual connections on learning. In: Thirty- first AAAI Conf Artif Intell. 2017.

116. He K, Zhang X, Ren S, et al. Deep residual learning for image recognition. In: Proceedings of the IEEE Conf Comput Vis Pat Recog. 2016:770–8.

117. Hasan AM, Jalab HA, Meziane F, Kahtan H, Ahmad AS. Combining Deep and Handcrafted Image Features for MRI Brain Scan Classification. IEEE Access; 2019. pp. 79959–79967.

118. Zaw HT, Maneerat N, Win KY. Brain tumor detection based on Naïve Bayes classification. Int Conf Eng Appl Sci Technol. 2019; pp.1–4.

119. Sert E, Ozyurt F, Doğantekin A. A new approach for brain tumor diagnosis system: Single image super resolution based maximum fuzzy entropy segmentation and convolutional neural network. Med Hypothes. 2019. pp. 1–9.

120. Deepak S, Ameer PM. Brain tumor classification using deep CNN features via transfer learning. Comput Biol Med. 2019. pp. 1–7.

121. Narayana TL, Reddy TS. An Efficient Optimization Technique to Detect Brain Tumor from MRI Images. Int Conf Smart Syst Invent Technol. 2018. pp. 1–4.

122. Polly FP, Shil SK, Hossain MA, Ayman A, Jang YM. Detection and Classification of HGG and LGG Brain Tumor Using Machine Learning. Int Conf Inform Network. 2018. pp. 813–817.

123. Amin J, Sharif M, Yasmin M, Fernandis S. A distinctive approach in brain tumor detection and classification using MRI. Pat Recog Lett. 2017. pp. 1–10.

124. Long J, Shelhamer E, Darrell T. Fully convolutional networks for semantic segmentation. In: Proceedings of the IEEE Conf Comput Vis Pat Recog. 2015:3431–40.

125. Everingham M, Van Gool L, Williams CKI, et al. The pascal visual object classes challenge 2012 (voc2012) results. Available online: http://www.pascal-network.org/challenges/VOC/voc2011/workshop/index.

126. Ronneberger O, Fischer P, Brox T. U-net: Convolutional networks for biomedical image segmentation. In: International

Conference on Medical image computing and computer-assisted intervention. Cham: Springer, 2015:234–41.

127. Badrinarayanan V, Kendall A, Cipolla R. SegNet: A deep convolutional encoder-decoder architecture for image segmentation. IEEE Trans Pattern Anal Mach Intell. 2017;39:2481–95.

128. Avizenna MH, Soesanti I., Ardiyanto I. Classification of Brain Magnetic Resonance Images based on statistical features. Int Conf Bioinform Biotechnol Biomed Eng. 2018. pp. 1–5.

129. Keerthana TK, Xavier S. An Intelligent System for Early Assessment and Classification of Brain Tumor. Proceedings of the 2nd Int Conf Inventive Commun Comput Technol. 2018. pp. 1–4.

130. Gupta N, Khanna P. A non-invasive and adaptive CAD system to detect brain tumor from T2-weighted MRIs using customized Otsu's thresholding with prominent features and supervised learning. Signal Process Image Commun. 2017. pp. 1–9.

131. Gupta N, Bhatele P, Khanna P. Identification of Gliomas from brain MRI through adaptive segmentation and run length of centralized patterns. J Comput Sci. 2017. pp. 1–8.

132. Minz A, Mahobiya C. MR Image classification using adaboost for brain tumor type. IEEE 7th Int Adv Comput Conf. 2017. pp. 1–5.

133. Taie SA, Ghonaim W. Title CSO-based algorithm with support vector machine for brain tumor's disease diagnosis. IEEE Int Conf Pervasive Comput Commun Workshops. 2017. pp. 1–5.

134. Shankar AS, Asokan A, Sivakumar D. Brain Tumor Classification Using Gustafson–kessel (G-k) Fuzzy Clustering Algorithm. Int J Latest Eng Res Appl. 2016. pp. 68–72.

135. Gumaei A, Hassan MM, Hassan MR, Alelaiwi A, Fortino G. A Hybrid Feature Extraction Method with Regularized Extreme Learning Machine for Brain Tumor Classification. IEEE Access. 2019. pp. 36266–36273.

136. Hemanth G, Janardhan M, Sujihelen L. Design and Implementing Brain Tumor Detection using Machine Learning Approach. Third Int Conf Trends Electron Infor. 2019. pp. 1–6.

137. Mallick PK, Ryu SH, Satapathy SK, Mishra S, Nguyen GN, Tiwari P. Brain MRI Image Classification for Cancer Detection Using Deep Wavelet Autoencoder Based Deep Neural Network. IEEE Access. 2019. pp. 46278- 46287.

138. Swati Z, Zhao Q, Kabir M, Ali F, Ahmed S, Lu J. Brain tumor classification for MR images using transfer learning and fine tuning. Comput Med Imag Graph. 2019. pp. 34–46.

139. Latif G, Iskandar DNF, Alghazo JM, Mohammad N. Enhanced MR Image Classification Using Hybrid Statistical and Wavelets Features. IEEE Access. 2018. pp. 9634- 9644.

140. Selvapandian A, Manivannan K. Fusion Based Glioma Brain Tumor Detection and Segmentation using ANFIS Classification. Comput Methods Programs Biomed. 2018. pp. 33–38.

141. Mohsen H, Sayed E, Dahshan E, Badeeh A, Salem M. Classification using deep learning neural networks for brain tumors. Future Comput Inform J. 2018. pp. 68–73.

142. Anaraki AK, Moosa A, Kazemi F. Magnetic resonance imaging-based brain tumor grades classification and grading via convolutional neural networks and genetic algorithms. Biocybern Biomed Eng. 2019. pp. 63–74.

143. Banerjee S, Mitra S, Shankar U. Synergetic NeuroFuzzy Feature Selection and Classification of Brain Tumors. IEEE Int Conf Fuzzy Syst. 2017. pp. 1–10.

144. Lavanyadev R, Machakowsalya M, NivethithaJ J, Kumar N. Brain Tumor Classification and Segmentation in MRI Images using PNN. Int Conf Electric Instrument Commun Eng. 2017. pp. 1–6.

145. Nazir M, Wahid F, Khan S. A simple and intelligent approach for brain MRI classification. J Intell Fuzzy Syst. 2015:1127–1135.